

## Synthesis, characterization and a.c. conductivity of polypyrrole/Y<sub>2</sub>O<sub>3</sub> composites

T K VISHNUVARDHAN, V R KULKARNI\*, C BASAVARAJA and S C RAGHAVENDRA<sup>†</sup>

Department of Chemistry, Gulbarga University, Gulbarga 585 106, India

<sup>†</sup>Department of Electrical and Computer Engineering, University Federal of Para, P O Box 8619, CEP 66075-900, Belem, Brazil

MS received 20 June 2005; revised 17 December 2005

**Abstract.** Conducting polymer composites of polypyrrole/yttrium oxide (PPy/Y<sub>2</sub>O<sub>3</sub>) were synthesized by *in situ* polymerization of pyrrole with Y<sub>2</sub>O<sub>3</sub> using FeCl<sub>3</sub> as an oxidant. The Y<sub>2</sub>O<sub>3</sub> is varied in five different weight percentages of PPy in PPy/Y<sub>2</sub>O<sub>3</sub> composites. The synthesized polymer composites are characterized by infrared and X-ray diffraction techniques. The surface morphology of the composite is studied by scanning electron microscopy. The glass transition temperature of the polymer and its composite is discussed by DSC. Electrical conductivity of the compressed pellets depends on the concentration of Y<sub>2</sub>O<sub>3</sub> in PPy. The frequency dependent a.c. conductivity reveals that the Y<sub>2</sub>O<sub>3</sub> concentration in PPy is responsible for the variation of conductivity of the composites. Frequency dependent dielectric constant at room temperature for different composites are due to interfacial space charge (Maxwell Wagner) polarization leading to the large value of dielectric constant. Frequency dependent dielectric loss, as well as variation of dielectric loss as a function of mass percentage of Y<sub>2</sub>O<sub>3</sub> is also presented and discussed.

**Keywords.** Composites; polypyrrole; conductivity; spectroscopy.

### 1. Introduction

Conducting polymers are important materials emerging with lot of applications in various fields. Research in the field of such polymers aims mainly at some suitable modifications of existing polymers so that their applicability can be improved. Some of these modifications involve preparing hybrid materials in which organic materials and inorganic oxides or salts of different metals, viz. SnO<sub>2</sub> (Bhattacharya *et al* 1996), CeO<sub>2</sub> (Galembeck and Oswald 1997), V<sub>2</sub>O<sub>5</sub> (Harreld *et al* 1999), TiO<sub>2</sub> (Su and Kuramoto 2000), fly ash composites (Raghavendra *et al* 2003), Fe<sub>3</sub>O<sub>4</sub> (Chen *et al* 2003), ZrO<sub>2</sub> (De *et al* 2004) etc combine in some special fashion with the conducting polymers to give rise to the composites. In almost all the cases some specific nature of association between the two components have been observed. Polypyrrole is an important conducting polymer with high electrical conductivity and appreciable environmental stability (Chen *et al* 1997).

Yttria stabilized zirconia shows good sensor application due to high operating temperature, which makes these oxide sensors suitable for automotive applications (Chiu *et al* 1992). A.C. electrical properties of conjugated polymers and theoretical high-frequency behaviour of multi

layer films have been studied by Lee *et al* (2001). The survey of literature reveals that the detailed conductivity studies on PPy/Y<sub>2</sub>O<sub>3</sub> composites are scarce. The present study deals with the synthesis, characterization of PPy/Y<sub>2</sub>O<sub>3</sub> composites and evaluation of a.c. electrical conductivity for different weight percentages of Y<sub>2</sub>O<sub>3</sub> in PPy composites. The characterization of the composites has been done by IR, XRD, SEM and DSC analysis techniques.

### 2. Experimental

#### 2.1 Materials

Anhydrous iron (III) chloride from Fischer (AR-grade), yttrium oxide from SD-Fine chemicals (AR-grade) and pyrrole from Fluka were obtained and used in the present study. Pyrrole monomer was purified by distillation under reduced pressure and stored at 4°C in the absence of light.

#### 2.2 Synthesis of PPy and PPy/Y<sub>2</sub>O<sub>3</sub> composites

Chemically polymerized polypyrrole and its yttrium oxide composites were obtained by oxidative polymerization by using FeCl<sub>3</sub> as oxidant in aqueous medium. 0.02 mole pyrrole monomer was added drop wise to the aqueous

\*Author for correspondence (vijaykumar2@sancharnet.in)

solution of 100 ml of  $\text{FeCl}_3$  (0.06 mole) solution. This approach promotes molecular level mixing of precursor and the polymerization of initiators of both networks. The oxide was varied in weight percentages of yttrium oxide (10, 20, 30, 40 and 50%) and added to the PPy solution. The reaction mixture was stirred for about 3 h in order to disperse yttrium oxide in the polymer solution. The purpose of oxidizing pyrrole was to complete the oxidative polymerization of unreacted pyrrole and achieve oxidative doping of PPy. As soon as the pyrrole mixed with the  $\text{FeCl}_3$  solution, it turned to characteristic black colour, indicating that the organic polymerization reaction began immediately. After 3 h of stirring, the hybrid of metal oxide and PPy was washed thoroughly with water. To remove last traces of unreacted pyrrole, it was then washed with methanol. Composites were vacuum dried at 60–70°C for 1 h.

### 3. Measurements

The composites thus obtained were characterized by infrared (FT-IR), X-ray diffraction (XRD) and scanning electron microscopic (SEM) techniques. The IR spectra of the composites were recorded in Perkin Elmer (model-1600 series UK) IR spectrometer in KBr medium at room temperature in the region 4000–450  $\text{cm}^{-1}$ . The X-ray diffraction pattern of the sample was recorded on Philips X-ray diffractometer using  $\text{CuK}_\alpha$  ( $\lambda = 1.5406 \text{ \AA}$ ). The diffractogram was recorded in terms of  $2\theta$  in the range 20–80°. The powder morphology of the PPy and PPy/ $\text{Y}_2\text{O}_3$  composite was investigated by using Philips XL-30 ESEM scanning electron microscopy. DSC studies for the above samples were also carried out by using a V2 6D TA instrument model DSC 2010. Initial scan was taken from 50–100°C to remove the thermal history effects, then cooled to 50°C under nitrogen atmosphere. Data collected at 10°/min, in the range of 273–873 K showed typical sample size for pure PPy as 2 mg, and that of the composite, 5 mg.

The powders of PPy and PPy/ $\text{Y}_2\text{O}_3$  so obtained were crushed and finely ground in agate mortar. The composite powders were pressed to form pellets of 10 mm diameter and 2–2.5 mm thickness by applying pressure of 90 MPa in hydraulic press. The pellets of PPy and its composites were coated with silver paste on either side. Copper electrodes were placed on both the surfaces to obtain a better contact. The electrical resistivity of PPy and PPy/ $\text{Y}_2\text{O}_3$  composites were measured using Hewlett–Packard impedance analyser 4191A in the frequency range  $10^2$ – $10^6$  Hz at room temperature.

The real part of relative dielectric constant was evaluated by the relation

$$C = \epsilon_1 \epsilon_0 A/t,$$

where  $\epsilon_0$  is the vacuum permittivity,  $A$  the area and  $t$  the thickness of the sample.

## 4. Results and discussion

### 4.1 FTIR spectra

Figure 1a shows FTIR spectrum of pure PPy. The bands at 1547 (2,5-substituted pyrrole) and 1452  $\text{cm}^{-1}$  may be assigned to typical polypyrrole ring vibrations. The bands at 1312, 1040  $\text{cm}^{-1}$  may correspond to =C–H band in plane vibration. The broad band at 1178  $\text{cm}^{-1}$  may be assigned for N–C stretching band (Nicho and Hu 2000). The IR peak observed at 889  $\text{cm}^{-1}$  may be assigned to the =C–H out of plane vibration indicating polymerization of pyrrole (Chen *et al* 2003). Figure 1b shows IR spectrum of  $\text{Y}_2\text{O}_3$  with a characteristic IR peak being observed at 415  $\text{cm}^{-1}$  which may be attributed to the presence of M–O bond in  $\text{Y}_2\text{O}_3$  (Ross 1972; Nakamoto 1986). Figure 1c shows IR spectrum of PPy/ $\text{Y}_2\text{O}_3$  (with 30 weight percentage) composite, which exhibits absorption peaks at 1554 and 1460  $\text{cm}^{-1}$  for typical pyrrole ring vibration and that of =C–H in plane vibration peaks at 1304, 1045  $\text{cm}^{-1}$ . A broad peak at 1177  $\text{cm}^{-1}$  is assigned as N–C stretching band and bands observed at 789, 913  $\text{cm}^{-1}$  for the presence of polymerized pyrrole and that of metal oxide band at 444  $\text{cm}^{-1}$ . The IR spectra of other composites (PPy with 10, 20, 30 and 40 wt % of  $\text{Y}_2\text{O}_3$ ) show similar absorption peaks without much variations in their stretching frequen-

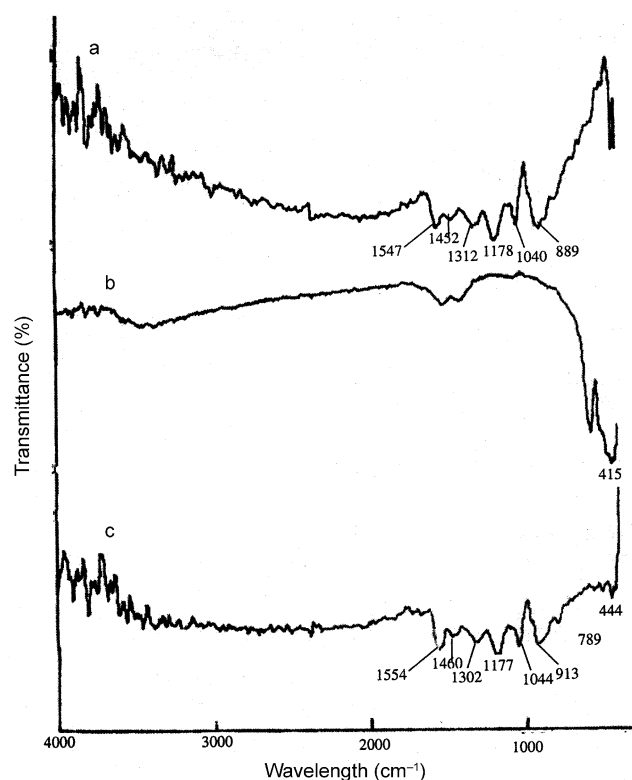


**Figure 1.** FTIR spectra of a. pure PPy, b.  $\text{Y}_2\text{O}_3$  and c. PPy/(30 wt %) of  $\text{Y}_2\text{O}_3$  composite.

cies. However, this may not exclude some weak interactions between the two components of the composite.

Patil *et al* (1988) reported that the temperature dependent IR data show the variations in the N–C stretching band indicating the presence of free electrons of the bipolarons pictured near the N–C bond in PPy. Due to the presence of bipolarons, charge hopping takes place through the chain so conduction continues.

#### 4.2 X-ray diffraction

Figure 2a presents X-ray diffraction pattern of pure PPy, which has a broad peak at about  $2\theta = 24.6^\circ$ , a characteristic peak of amorphous polypyrrole (Partch *et al* 1991). Figure 2b presents XRD pattern of pure Y<sub>2</sub>O<sub>3</sub>, characteristic peaks are indexed by lattice parameter values. Figure 2c presents XRD pattern of PPy/Y<sub>2</sub>O<sub>3</sub> (with 30 weight %) composite revealing the partial amorphous nature.

The broad peak is due to the scattering from PPy chains at the interplanar spacing (Ouyang and Li 1997). The appearance of the sharp peaks both in the pure oxide as

well as in the composite may indicate some degree of crystallinity in the composite. The sharp peaks in the pure oxide as well as composite well matches with the JCPDS file No. 43-0661. The average crystallite size of the pure oxide is calculated by using the Scherrer's formula,

$$D = Kl/b \cos q,$$

where  $D$  is crystallite size of particle,  $l = 1.54 \text{ \AA}$  being the X-ray wavelength of Cu  $K\alpha$  and  $K$  the shape factor, which can be assigned a value of 0.89 if the shape is unknown,  $\cos q$  the cosine of the Bragg angle and  $b$  the full width at half-height of angle of diffraction in radians. The above equation when introduced for the characteristic (111 plane) peak of Y<sub>2</sub>O<sub>3</sub> viz. at  $2\theta = 28.5$ , leads to about 100 nm. An average particle size of about 100 nm could be obtained by considering the intense characteristic peak (of 111 plane).

Diffraction pattern of the composite (in the 30 weight % of oxide) is the same as Y<sub>2</sub>O<sub>3</sub> as well as PPy. This means that PPy deposited on the surface of Y<sub>2</sub>O<sub>3</sub> particles

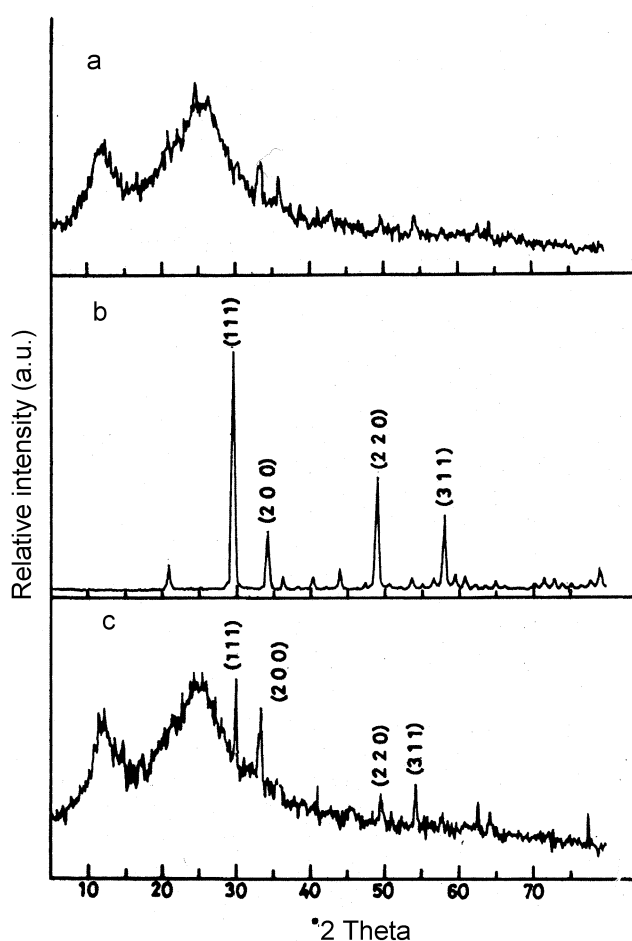


**Figure 2.** XRD patterns of a. pure PPy, b. Y<sub>2</sub>O<sub>3</sub> and c. PPy/(30 wt %) of Y<sub>2</sub>O<sub>3</sub> composite.

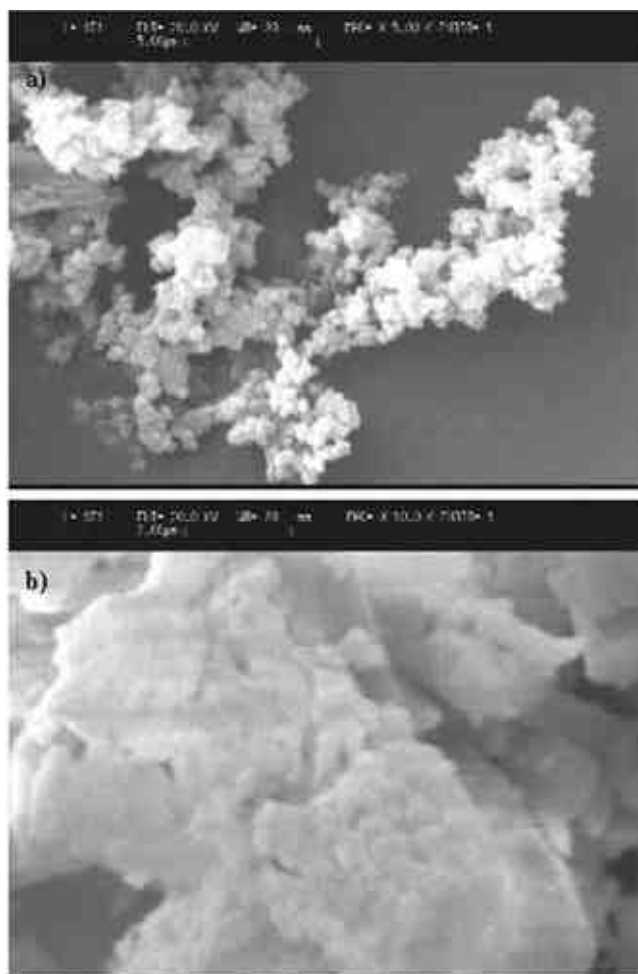


**Figure 3.** SEM of PPy/(30 wt %) Y<sub>2</sub>O<sub>3</sub> composites and pure Y<sub>2</sub>O<sub>3</sub>.

has little effect on crystallization performance of  $Y_2O_3$ . But as the oxide percentage increases in the composite, deposited PPY has no effect on the crystallization of  $Y_2O_3$  particles (Li *et al* 2003). It also implies that the composite is a more ordered arrangement than PPY at higher concentration of oxide (50 weight %) in the composite. This can be further confirmed from DSC plots.

#### 4.3 Scanning electron microscopy

Figures 3a and b show SEM of PPY/ $Y_2O_3$  (with 30 wt % of  $Y_2O_3$  in PPY) composite and pure  $Y_2O_3$ . A very high magnification of SEM images shows the presence of hemispherical nature of polymer as clusters in the composite. Oxide particles are covered by spherical nature of polypyrrole to form multiparticle aggregates, presumably because of weak interparticle interactions.

#### 4.4 Differential scanning calorimetry

Figure 4a shows DSC plot of pure PPY, having a broad endothermic dip at  $97.32^\circ\text{C}$ , which may be the glass transition temperature for pure PPY (overlapping the moisture release as well explained by Balci *et al* 1998). In case of figure 4b, for the PPY/ $Y_2O_3$  (30 weight %) composite, there is a corresponding steep dip at higher temperature

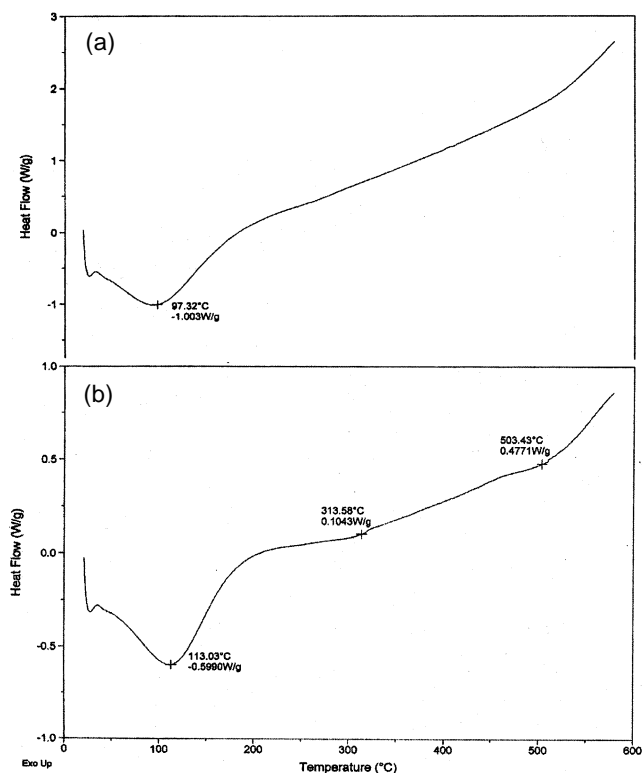


**Figure 4.** DSC plots of (a) pure PPY and (b) PPY/(50 wt %)  $Y_2O_3$  composite.

viz. at  $113.3^\circ\text{C}$ . It also contains few more inflection points: The one at  $313.58^\circ\text{C}$  may be due to the melting of PPY chain, the other at  $503.43^\circ\text{C}$  may be due to phase change of  $Y_2O_3$ .

There is no observable shoulder in the pure PPY as compared to the composite, indicating less orderness of the polymer molecules in the absence of oxide in the polymer. So they can attain the maximum vibration of molecules at equilibrium at higher temperature (i.e. glass transition temperature in the case of composite) in case of composite. Increase in the glass transition temperature in the composites may have two probabilities: One may be the attainment of the longer chain length due to the addition of oxide and other may be due to weak interactions of PPY and oxide in the more ordered system of the composite. First probability may be less likely due to the nearly same stretching frequencies obtained in the FTIR for pure PPY as well as for PPY/ $Y_2O_3$  composite. If chain length is varied, FTIR might have given different stretching frequencies in the composite. So, as FTIR did not show much variation in their stretching frequencies for the pure PPY and the composite, it implies weak interaction and more ordered arrangement of the polymer and the oxide.

#### 4.5 A.C. electrical conductivity

The frequency dependent electrical conductivities of PPY/ $Y_2O_3$  composites have been presented in figure 5. Inset of figure 5 indicates the frequency dependent electrical conductivity for pure PPY. The most important and interesting observation is that, the a.c. conductivity of all composites is significantly higher than the bare polymer, in spite of the fact that  $Y_2O_3$  is an insulating material at room temperature ( $5.9 \times 10^{-10}$  S/cm). For example, the bulk conductivity of pure PPY was measured to be about  $1.26 \times 10^{-4}$  S/cm

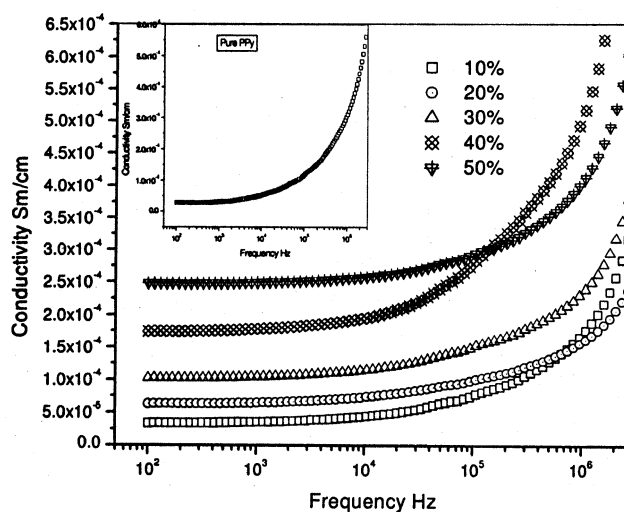


**Figure 5.** Frequency dependence of conductivity of PPY/ $Y_2O_3$  composite for various wt % of  $Y_2O_3$  (Inset: for pure PPY).

at  $10^5$  Hz, whereas for the 50 weight % composite, it is  $2.93 \times 10^{-4}$  S/cm. It is also found that conductivity is larger for larger weight % of  $Y_2O_3$  in the polymer composite. This is evident from figure 6, wherein, the conductivity is plotted as a function of weight % of yttrium oxide for some selected frequencies.

Further almost all the composites show similar behaviour up to  $10^5$  Hz, viz. that there is not much variation in the conductivity with frequency during this range. On the other hand, as the frequency is increased further, conductivity goes on increasing and the conductivities of all the composites merge together indicating the formation of excess charge carriers (polaron and bipolaron) at higher frequencies.

The total conductivity of the composite may depend on the microscopic and macroscopic conductivities. The microscopic conductivity depends upon the doping level, conjugation length or chain length etc, whereas the macroscopic conductivity depends on the inhomogeneities in the composites, compactness of pellets, orientation of microparticles etc. The PPy/ $Y_2O_3$  composite is inhomogeneous because of dispersion of  $Y_2O_3$  particles in the polymer composites. In the present study, composites are synthesized in identical conditions by *in situ* polymerization of pyrrole in the presence of  $Y_2O_3$ . So the microscopic conductivities remain almost the same but the physical (macroscopic) properties viz. compactness and molecular orientations, may significantly vary due to the variation in the weight % of  $Y_2O_3$  in the composites. Microcrystalline nature of oxide particles may give rise to increase in the orderness in the composites, which is confirmed from XRD and DSC. This orderness increases the compactness and molecular orientations leading to an increase in macroscopic conductivity.

The trend of the conductivities of conducting polymer/oxide composites is also same in case of polyaniline/fly

ash (Raghavendra *et al* 2003). They explained conductivity on the basis of the electron hopping mechanism. In all their studies there is not much variation in the conductivity. In fact, the conductivity decreases by small magnitude as the frequency is increased. On the other hand, the increase in conductivities observed by Bhattacharya *et al* (1996) for the case of  $ZrO_2$  sol dispersed in the polypyrrole matrix was accounted due to improved weak links between the grains, resulting in stronger coupling through the grain boundary.

Pure PPy is very light with poor compactness, the microparticles are randomly oriented and the linkage among the polymer particles through the grain boundaries is very poor resulting in relatively lower conductivity (Rupali and De 1999). The presence of  $Y_2O_3$  (heavier than PPy particles) in the composites helps to acquire a granular shape, which leads to an improvement in the compactness of the composite material. As the  $Y_2O_3$  content in the composites is increased, the change in compactness becomes more significant as a result of increasingly improved weak links between the grains and coupling through the grain boundaries becomes stronger, which ultimately results in the improvement in the macroscopic conductivity. Therefore, the conductivity of PPy/ $Y_2O_3$  composites is higher than the pure PPy. Aguilar-Hernandez and Potje-Kamloth (2001) and Singh (1991) accounted for the frequency dependent conductivity behaviour due to two mechanisms expressed as

$$s(w) = s_{a.c.}(w) + s_{d.c.}$$

The above equation represents the total conductivity in the context of the theory of relaxation processes in dielectric materials (Jonscher 1976, 1983) which is a classical way of studying a.c. conductivity in conducting polymers. The main idea relies on the separate processes. The total measured conductivity at a given frequency is separated into  $s_{a.c.}(w)$  and  $s_{d.c.}$  which is simply the limit of  $s_{a.c.}(w)$  when  $w \rightarrow 0$ . From figure 5 it is evident that at lower frequency, conductivity is independent of frequency but may be dependent on temperature.

#### 4.6 Dielectric behaviour

Dependence of dielectric constant and dielectric loss as a function of frequency ranging from 100– $10^6$  Hz at room temperature for the pure PPy and its composites is plotted in figures 7 and 8, respectively. The inset of figure 7 shows dielectric constant as a function of frequency for pure PPy. In both the cases of pure PPy as well as the composites, the dielectric constant shows steep decrease from its initial higher values. Above  $10^4$  Hz the dielectric constant remains nearly the same.

In a similar fashion figure 8 shows that the dielectric loss also decreases steeply as frequency increases. It can

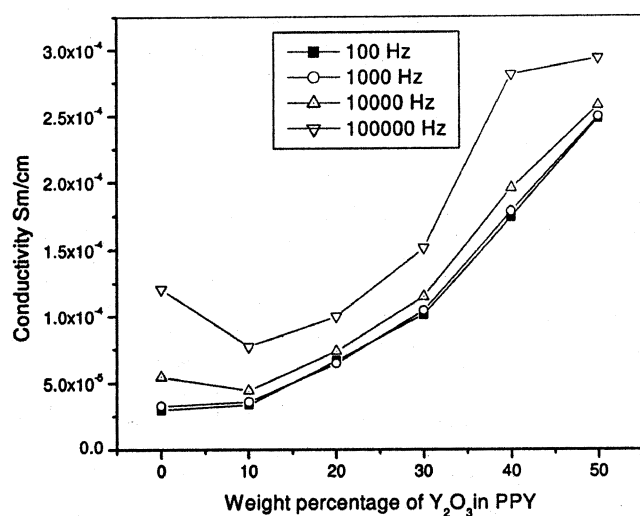


**Figure 6.** The conductivity of PPy/ $Y_2O_3$  composites for different wt % of  $Y_2O_3$  at different frequencies.

be observed that, dielectric constant as well as dielectric loss values are higher for the higher content of the oxide in the composite. When the dielectric behaviour is compared with conductivity behaviour of figures 5 and 6, it can be noted that the behaviour is opposite. Table 1 presents the representative values of dielectric constant as well as dielectric loss at two frequencies (i.e. 100 and  $10^6$  Hz) for the composite samples for which measurements were made.

At 100 Hz, the dielectric constant for the composite samples with 50 weight % of oxide is about 28,500. This value decreases to about 12,500 for the composite samples having 10 weight % of oxide. On the other hand, the value of the dielectric constant for pure PPy at this frequency is about 25,900.

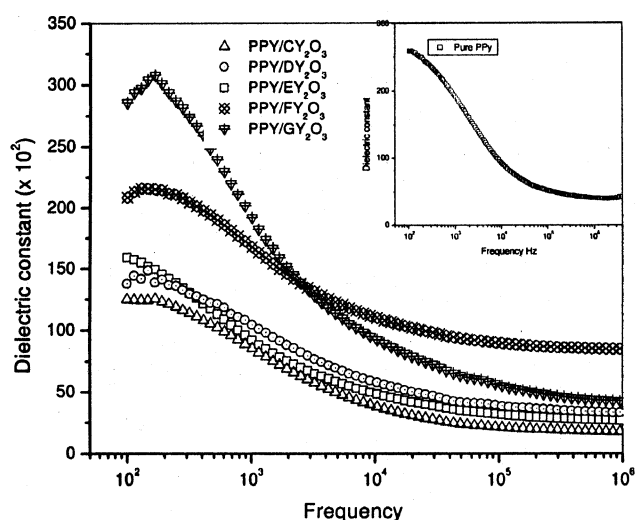


**Figure 7.** Frequency dependence of dielectric constant and PPy/ $Y_2O_3$  composites (inset: for pure PPy).

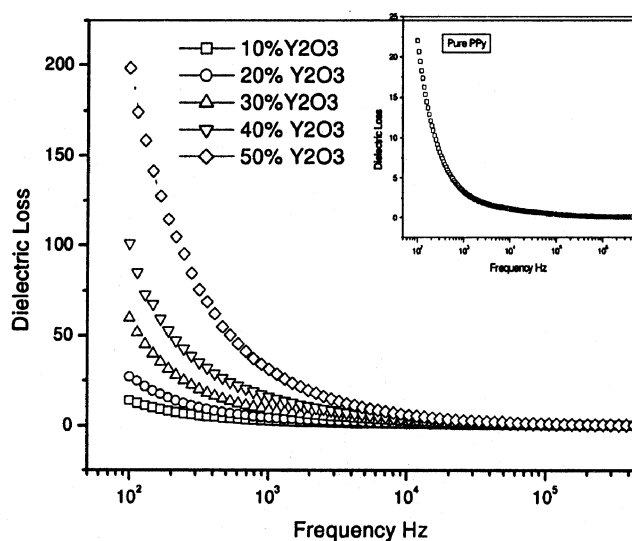


**Figure 8.** The frequency dependence of dielectric loss of PPy/ $Y_2O_3$  composites (inset: for pure PPy).

The corresponding dielectric loss for the composite samples with 50 weight % of oxide is about 198 at 100 Hz frequency. The value decreases to about 13 for the composite with 10 weight % of oxide. Similarly, the value of dielectric loss for pure PPy is about 20 at same frequency.

Dey *et al* (2005) reports similar trend in the dielectric behaviour of PPy/ $Fe_3O_4$  composites. They obtained maximum dielectric constant of about 11,000 for highest polymer content, but this decreases significantly with frequency. This value decreases with increase of  $Fe_3O_4$  and is almost independent of frequency. They observed highest value of dielectric constant of  $\sim 1000$  for pure PPy.

Mallikarjuna *et al* (2005) explained the dielectric behaviour for Pani/ $g-Fe_2O_3$  composites. He observed highest dielectric constant value of 5500 for 10 weight % of  $g-Fe_2O_3$ , which is higher than pure  $g-Fe_2O_3$  and pure Pani. He accounted for the highest dielectric constant due to high packing density of  $g-Fe_2O_3$  in Pani.

They compared the steep decrease in dielectric constant of composite with pure  $g-Fe_2O_3$  and accounted for loss of dielectric polarization and the polymer is in a higher reduced state due to the presence of higher hydrogen atoms. These hydrogen atoms could participate in the partial reduction of  $Fe^{3+}$  ions in an octahedral position of  $Fe_3O_4$  particles, thereby creating  $Fe^{2+}$  and  $Fe^{3+}$  ions. Thus reduction of  $Fe^{3+}$  ions might have increased at higher frequency, thereby producing the possible intermediate compositions. These intermediate compositions contribute to the decrease in dielectric constants.

As our composite samples are heterogeneous, dielectric constant may arise due to interfacial and space charge polarization at frequency from 100 Hz to M Hz. At lower frequency the dipole can respond rapidly to follow the field and dipole polarization has its maximum value, so highest dielectric constant and dielectric loss. At higher frequencies dipole polarizability will be minimum, as the field cannot induce the dipole moment, so dielectric values attain minimum.

Higher dielectric constant and dielectric loss for higher content of oxide, which may be due to increase in oxide, increases the crystallinity (as revealed from XRD). As a result orderliness increases (as revealed from DSC), the

**Table 1.** Composition effect on dielectric properties.

Percentage of oxide	Dielectric constant		Dielectric loss	
	at 100 Hz	at 1000 Hz	at 100 Hz	at 1000 Hz
0% oxide (pure PPy)	25967	19097	21.687	3.287
10% $Y_2O_3$	12508	8540.6	13.951	2.822
20% $Y_2O_3$	13780	9224.8	27.054	4.524
30% $Y_2O_3$	15941	10451	59.626	8.886
40% $Y_2O_3$	20850	16767	101.075	16.283
50% $Y_2O_3$	28584	19189	198.266	31.638
Pure $Y_2O_3$	5.084	8.5069	0.653	0.114

interfacial interactions between the polymer and Y<sub>2</sub>O<sub>3</sub> lead to maximum space charge polarization (Maxwell 1998). In Maxwell Wagner two-layered model, the dielectric function depends on the conductivity and permittivity of the two layers. The dielectric constant arises due to static dielectric permittivity, which can be given as

$$\epsilon_s = C_{gb}/C_0.$$

The above equation demonstrates that the dielectric constant mainly depends on the grain boundary capacitance. The grain conductivity decreases with increase in Y<sub>2</sub>O<sub>3</sub> concentration, the charge carrier concentration decreases resulting in a decrease in grain boundary capacitance. The grain size also decreases with increasing Y<sub>2</sub>O<sub>3</sub> content. Hence the reduction of grain boundary capacitance and grain size gives rise to a decrease in dielectric constant.

For pure PPy, highest conductivity and dielectric loss behaviour may be due to the free motion of the charge carriers. In case of composites, while oxide content is less (i.e. 10%) in the polymer the interface between the polymer and grain is poor leading to decrease in conductivity and dielectric behaviour. As the oxide content is more (i.e. 50%) in the polymer composite, orderliness increases, so packing density increases, interface between the polymer and oxide is more leading to maximum space charge polarization (Maxwell Wagner polarization) contributing to highest dielectric behaviour.

## 5. Conclusions

PPy/Y<sub>2</sub>O<sub>3</sub> composites are prepared by dispersing different amounts of Y<sub>2</sub>O<sub>3</sub> particles in polypyrrole matrix. The FTIR spectral peaks of PPy/Y<sub>2</sub>O<sub>3</sub> composite (with 30 weight % Y<sub>2</sub>O<sub>3</sub>) shows presence of oxide in the polymer though Y<sub>2</sub>O<sub>3</sub> in the composites does not effectively involve chemically with PPy. But weak interaction with oxide and PPy may contribute to the conductivity and dielectric behaviour. The XRD study reveals the encapsulation of oxide particles by polymer and some degree of crystallinity. SEM images of PPy/Y<sub>2</sub>O<sub>3</sub> show aggregation of particles as well as particles agglomeration. The DSC plots further supplements the weak interactions of the polymer with the oxide particle and thermal stability. DSC and XRD show increased orderliness in the polymer composite than in the pure PPy. The increase in the a.c. electrical conductivity of the PPy/Y<sub>2</sub>O<sub>3</sub> composites over pure PPy is due to macroscopic conductivity. PPy/Y<sub>2</sub>O<sub>3</sub> composites with higher weight percentage of Y<sub>2</sub>O<sub>3</sub> show higher conductivity than pure PPy due to increased orderliness in the composites. Frequency dependent dielectric constant is on the basis of the dielectric mechanism. Increase in the values of the dielectric behaviour may be due to interface between the oxide and the polymer increases the orderliness and the packing density and maximum space charge (Maxwell Wagner) polarization may occur. Dielectric loss arises due to the localized motion of the charge carriers. Highest

dielectric behaviour is possible for application in conductive paints, rechargeable batteries, sensors and actuators etc.

## Acknowledgements

Authors are thankful to Prof. K B R Varma, Materials Research Centre, Indian Institute of Science, Bangalore, for providing facilities. Authors are also thankful to Dr M V N Ambika Prasad, Department of Physics, Gulbarga University, Gulbarga, for useful discussions.

## References

- Aguilar-Hernandez J and Potje-Kamloth K 2001 *J. Phys. D: Appl. Phys.* **34** 1700
- Balci N, Akbulut U, Toppare L, Stanke D and Hallensleben M L 1998 *Tr. J. Chem.* **22** 73
- Bhattacharya A, De S, Bhattacharya S N and Das S 1994 *J. Phys. Cond. Matter* **6** 10499
- Bhattacharya A, Ganguly K M, De A and Sarkar S 1996 *Mater. Res. Bull.* **31** 527
- Chen W, Xingwei L, Gi X, Zhaoquang W and Wenqing Z 2003 *Appl. Surf. Sci.* **218** 216
- Chen X B, Issi J P and Devaux J 1997 *J. Polym. Sci.* **32** 1515
- Chiu H T, Lin S J and Huang C M 1992 *J. Appl. Electrochem.* **22** 358
- De Amitabha, Ajay D and Susanta L 2004 *Synth. Met.* **144** 303
- Dey Ashis, De Amitabha and De S K 2005 *J. Phys. Cond. Matter* **17** 5895
- Galembeck A and Oswald L A 1997 *Synth. Met.* **84** 151
- Harreld J H, Dunn B and Nazar L F 1999 *Int. J. Inorg. Mater.* **1** 135
- Jonscher A K 1976 *Thin Solid Films* **36** 1
- Jonscher A K 1983 *Dielectric relaxation in solids* (London: Chelsea Dielectric) p. 86
- Lee C Y, Kim H M, Park J W, Gal Y S, Jin J I and Joo J 2001 *Synth. Met.* **117** 109
- Li Xingwei, Chen Wei, Bian Chaoqing, He Jinbo, Xu Ning and Xue Gi 2003 *Appl. Surf. Sci.* **217** 16
- Mallikarjuna N N, Manohar S K, Kulkarni P V, Venkataraman A and Aminabhavi T M 2005 *J. Appl. Polym. Sci.* **97** 1868
- Maxwell J C 1998 *A treatise on electricity and magnetism* (Oxford: Oxford University Press) **1**
- Nakamoto K 1986 *Infrared and Raman spectra of inorganic and coordination compounds* (New York: Wiley) 4th edn, p. 132
- Nicho M E and Hu H 2000 *Solar Energy Materials and Solar Cells* **63** 423
- Ouyang J and Li Y 1997 *Polymer* **38** 3997
- Partch R E, Gangoli S G, Matijevic E, Cai W and Aarajs S 1991 *J. Colloid. Interface Sci.* **27** 144
- Patil A O, Heeger A J and Wudl F 1988 *Chem. Rev.* **88** 183
- Ross S D 1972 *Inorganic infrared and Raman spectra* (London: McGraw Hill) 3rd edn, p. 107
- Raghavendra S C, Khasim S, Revanasiddappa M, Ambika Prasad M V N and Kulkarni A B 2003 *Bull. Mater. Sci.* **26** 733
- Rupali Gangopadhyay and De Amitabha 1999 *Euro Polym. J.* **35** 1985
- Singh R, Tandon R P, Panwar V S and Chandra S 1991 *J. Appl. Phys.* **69** 2504
- Su Shi-Jain and Kuramoto N 2000 *Synth. Met.* **114** 147